Anthocyanin contents and molecular changes in rose petals during the post-anthesis color transition

Ying Kong[1,2], Huan Wang[1,2], Li Qiu[3], Xiaoying Dou[1,2], Lixin Lang[1] and Jinrong Bai[1,2*]

[1] *Institute of Radiation Technology, Beijing Academy of Science and Technology, Beijing 100875, China*
[2] *Key Lab of Beam Technology and Material Modification of Ministry of Education, College of Nuclear Science and Technology, Beijing Normal University, Beijing 100875, China*
[3] *Beijing Botanical Garden Management Office, Beijing 100093, China*
* Corresponding author, E-mail: bjr301@126.com

Abstract

Flower color transitions during anthesis are taxonomically widespread; however, the mechanisms underlying post-anthesis color transition in roses are unclear. In this study, we collected petals of the butterfly rose (*Rosa chinensis* 'Mutabilis'), a post-anthesis color change cultivar, at different developmental stages and under different treatments. Anthocyanin composition and transcriptome data were analyzed to identify the environmental factors and crucial genes involved in post-anthesis color transition. The results showed that sunlight is a key factor triggering color transition. In butterfly rose flowers, color transition results from an increase in the accumulation of anthocyanins, primarily cyanidin-3-*O*-glucoside, and cyanidin-3,5-*O*-diglucoside. A combination of genome-wide identification, RNA-seq analysis, bioinformatics analysis, and quantitative real-time PCR verification revealed that *RcUF3GT1* and *RcGSTF2* genes were involved in anthocyanin production and anthocyanin transport, respectively. *RcMYB114a* may play a significant role in anthocyanin biosynthesis during color transition in roses, and *RcBBX28* might be a crucial gene involved in this process. These insights contribute to our knowledge of flower color change and have implications for further research on plant genetics and flower color evolution.

Introduction

Flower color change during anthesis, or post-anthesis color change (PACC), is a widespread and natural phenomenon, distinct from simple flower degeneration[1,2]. PACC is generally considered an adaptive signal indicating floral suitability to pollinators by redirecting pollinators to a close range while maintaining long-distance attraction to the plant's floral display[3,4]. PACC is also a favorable trait for horticultural plants as the retention of post-change older flowers enhances floral display size and prolongs the ornamental period.

PACC is associated with changes in flower pigment composition, primarily of carotenoids and anthocyanins[5]. Color changes resulting from changes in carotenoid content mainly lead to minor hue changes in yellow and white flowers, such as *Lonicera japonica*[6]. Conversely, more striking color transitions are often accompanied by shifts in anthocyanin composition. Many plants exhibit PACC because of an increase or decrease in anthocyanin content, resulting in significant color changes; for example, the post-anthesis transition in flower color from white to red in *Hisbiscus mutabilis*[7], white to pink in *Nicotiana mutabilis*[8], white to purple in *Viola cornuta* 'Yesterday, Today and Tomorrow'[9], yellow to red in *Lotus filicaulis* and *Rosa hybrida* 'Ehigasa'[1,10], and purple to white in *Brunfelsia acuminata*[11]. Sunlight and pollination are critical environmental triggers for color changes[9]. For example, petal color change in *Quisqualis indica* was induced by light[12], and pollination significantly accelerated PACC in *Lotus filicaulis* and *Euphrasia dyeri*[1,13].

The biosynthetic pathway and transcriptional regulation of anthocyanins in plants are well documented[14,15], and many structural genes involved in the anthocyanin biosynthesis pathway have been identified in roses[16]. Several transcription factors associated with the regulation of the anthocyanin biosynthetic pathway have also been characterized, and three MYB-bHLH-WD40 (MBW) complexes (RcMYB1-RcbHLH42-RcTTG1, RcMYB1-RcEGL1-RcTTG1, and MYB114a-bHLH3-WD40) have been linked to anthocyanin accumulation[17,18]. Other transcription factors, such as B-box zinc finger (BBX), NAC (NAM, ATAF, and CUC), and WRKY, also affect the transcriptional regulation of anthocyanin biosynthesis in Rosaceae plants[19–21].

Anthocyanins are biosynthesized on the cytoplasmic surface of the endoplasmic reticulum and transported into the vacuole for storage[22]. Many anthocyanin transport genes have been identified, including ATP-binding cassette (ABC), multidrug and toxic compound extrusion (MATE), and glutathione *S*-transferase (GST) genes[23]. Various GSTs function as anthocyanin transporters in plants, such as *ZmBZ2* in maize (*Zea mays*)[24], *PhAN9* in petunia (*Petunia hybrida*)[25], *AtTT19* (*AtGSTF12*) in *Arabidopsis thaliana*[26], *CkmGST3* in cyclamen (*Cyclamen* 'Kaori-no-mai')[27], *PpRiant* (*PpGST1*) in peach (*Prunus persica*)[28,29], *VvGST4* in grapevine (*Vitis vinifera*)[30], *LcGST4* in litchi (*Litchi chinensis*)[31], *FvRAP* in strawberry (*Fragaria vesca*)[32], *CsGSTF1* in purple tea (*Camellia sinensis*)[33], *IbGSTF4* in *Ipomoea batatas*[34], *MdGSTF6* in apple (*Malus* × *domestica*)[22], and *MtGSTF7* in *Medicago truncatula*[35], most of which belong to the Phi(F)

class. Additionally, some plant ABC and MATE genes are involved in anthocyanin transport, including *ZmMRP3* in maize[36], *VvABCC1*, *VvAM1* and *VvAM3* in grapevine[37,38], *OsMRP15* in rice (*Oryza sativa*)[39], *AtABCC2* and *AtTT12* in *A. thaliana*[40,41], *CaMATE1* in chickpea (*Cicer arietinum*)[42], *SlMTP77* in tomato (*Solanum lycopersicum*)[43], and *MtMATE2* in *M. truncatula*[44].

Roses (*Rosa* spp.) are ornamental plants with global economic importance. Some rose cultivars exhibit a post-anthesis transition from yellow to red/orange-red, such as the flowers of *R. hybrida* 'Masquerade'[45], *R. hybrida* 'Ehigasa' and 'Charleston'[46], *R. hybrida* 'Spectra'[47], and *R. hybrida* 'Chen Xi'[48]. The flower color change in 'Ehigasa' and 'Charleston' rose is attributed to the accumulation of anthocyanins, and the flowers of 'Chen Xi' and 'Spectra' do not turn red under shading conditions[46−48]. However, the mechanisms underlying post-anthesis color transition in roses are unclear. The butterfly rose (*R. chinensis* 'Mutabilis') is an ancient Chinese rose cultivar with single petals that change from light yellow to pink or dark pink during four-day anthesis. In this study, high-performance liquid chromatography-diode array detection (HPLC-DAD) and transcriptome analyses of butterfly rose samples were employed to determine the anthocyanin composition and molecular changes during PACC and identify the environmental factors influencing the PACC trait. This research offers a comprehensive analysis of the PACC trait in roses, as well as valuable information for understanding flower color evolution.

Materials and methods

Plant materials and sample collection

Samples of butterfly rose were collected from Kunming Yang Chinese Rose Gardening Co., Ltd., and planted in the germplasm garden of the Institute of Radiation Technology (116°43' N, 40°16' E) under open field conditions for 2–3 years. The PACC cultivar *R. hybrida* 'Spectra' was used for to verify candidate genes. *Rosa hybrida* 'Spectra' was cultivated in the China National Botanical Garden (North Garden). The collection of petal samples was authorized.

Different floral developmental stages of butterfly rose flowers, namely the bud stage (one day before anthesis, S3), first day of anthesis (D1), second day of anthesis (D2), third day of anthesis (D3), and fourth day of anthesis (senescent flowering stage, D4), were collected from the upper half of the petals between 08:00 and 09:00 on sunny days. More than 30 flowers were collected at each stage. Petal samples with additional anthocyanin coloration on the abaxial surface were excluded. The red part (post-change, SR) and yellow part (pre-change, SY) of the middle-layer petals of *R. hybrida* 'Spectra' were collected on the fourth or fifth day of anthesis in the morning (equivalent to the D2 stage of butterfly rose). The samples were collected from more than 15 *R. hybrida* 'Spectra' flowers. The fresh petal samples were cut, weighed, and immediately frozen in liquid nitrogen. Three biological replicates were collected, and samples were frozen and stored at −80 °C.

Sample treatments

Different treatments were used in this study to investigate the effects of light on butterfly rose petals, with buds about to open wrapped in different bags in the evening until the second day of anthesis (08:00–09:00) before flowering. First, paper bag treatment (PT) with semi-translucent paper bags (sketch tracing paper, Rotring, 78% light transmittance) was used under natural light–dark conditions. Second, aluminum foil bags were used for dark treatment (DT)[49]. Petals were sampled in the morning on the second day of anthesis. Additionally, in the afternoon (17:30) on the first day of anthesis, the flowers (equivalent to stage D1.5) were wrapped in aluminum foil bags until the next morning (08:00–09:00) (D1.5–2), and the petals of stages D1.5 and D1.5–2 were collected. More than 30 flowers were included under PT and DT, with more than 15 flowers collected from D1.5 and D1.5–2. D2 samples, which were opened under natural sunlight, were used as controls.

Measurement of anthocyanins

Anthocyanins were extracted according to the methods described by Wan et al.[50]. Approximately 0.1 g (fresh weight) of the sample was ground into a powder, transferred into a centrifuge tube, and extracted overnight at 4 °C using a 2 mL mixture of methanol:water:methane acid:trifluoroacetic acid (70:27:2:1, v/v/v/v). The extracts were centrifuged at $10,000 \times$ g and 4 °C for 10 min, and the supernatants were collected and filtrated (PTFE, 0.22 μm, Anpel). HPLC-DAD analysis was performed using an Agilent 1200/G1315D system in the wavelength range of 200–700 nm. The mobile phases comprised 0.5% aqueous formic acid (A) and acetonitrile (B). The gradient program has previously been described by Wan et al.[51]. A Zorbax SB-C18 analytical column (250 mm × 4.6 mm, 5 μm) was used. The column temperature, injection volume, and flow rate were set at 25 °C, 20 μL, and 0.5 mL/min, respectively. Anthocyanins were detected at a wavelength of 520 nm. In preliminary experiments, the anthocyanin composition was analyzed using ultra-performance liquid chromatography-electrospray tandem mass spectrometry (ExionLC AD; MS, Applied Biosystems 6500 Triple Quadrupole) using mixed petals at different developmental stages. Eight major anthocyanin components were identified. Anthocyanins were quantitatively analyzed using an external standard method[50]. Five anthocyanin standards, including cyanidin-3,5-O-diglucoside (Cy3G5G), cyanidin-3-O-glucoside (Cy3G), peonidin 3,5-O-diglucoside (Pn3G5G), peonidin 3-O-glucoside (Pn3G), and pelargonidin-3-O-diglucoside (Pg3G), were purchased from Sigma-Aldrich Chemical Co., Inc. (St. Louis, MO, USA). The remaining anthocyanins were quantified using a Cy3G standard curve.

Genes involved in anthocyanin biosynthesis in *R. chinensis*

According to the literature and our previous work, we identified 16 structural genes (excluding the UDP-glycosyltransferase family) involved in the flavonoid/anthocyanin biosynthetic pathway (Supplemental Table S1)[16]. The hidden Markov model profile PF00201 was used to search the rose genome for genes belonging to UDP glycosyltransferases (UGT), with an E-value of < 0.001, resulting in 217 candidate UGT genes[52]. Several transcription factor families involved in the regulation of anthocyanin biosynthesis have been identified in the rose genome, including 121 R2R3-MYB[53], 187 WD40[54], 100 bHLH[55], 48 basic leucine zipper (bZIP)[56],116 NAC[57], and 56 WRKY genes[58]. In addition, 23 BBX genes were re-identified in the rose genome based on a previous study[59].

Identification and analysis of GSTs in *R. chinensis*

The hidden Markov model profiles PF02798 (GST_N) and PF00043 (GST_C), downloaded from the Pfam website[60], were

used to identify candidate GSTs in *R. chinensis* with an E-value of < 0.001. Additionally, 65 *AtGST* sequences (Supplemental Table S2) were downloaded from the genome of *A. thaliana*[61] and used as a query to search for candidate GSTs in the *R. chinensis* genome (https://lipm-browsers.toulouse.inra.fr/pub/RchiOBHm-V2/) using the BLASTp program with an E-value cutoff of 1e−5. All non-redundant *RcGST* candidate genes were further verified by submission to the SMART website (http://smart.embl.de/)[62]. The *AtGST* gene family contained 12 conserved motifs (E-value < 0.001), including GST_N (PF02798), GST_N_2 (PF13409), GST_N_3 (PF13417), GST_N_4 (PF17172), GST_C (PF00043), GST_C_2 (PF13410), GST_C_3 (PF14497), GST_C_6 (PF17171), EF1G (PF00647), Glutaredoxin (PF00462), Hemerythrin (PF01814), and membrane-associated proteins in eicosanoid and glutathione metabolism (MAPEG; PF01124) (Supplemental Fig. S1)[63]. Candidate *RcGSTs* and 65 *AtGSTs* were used to construct a neighbor-joining phylogenetic tree. *RcGSTs* in the same subfamily with the same domain(s) as *A. thaliana* were identified as full-length GST genes, whereas those with incomplete domain(s) were identified as partial GST (GST-p) genes (Supplemental Fig. S2).

The identified full-length *RcGST* protein sequences were aligned using MAFFT 7.0 with default parameters[64], and phylogenetic trees were constructed using the maximum likelihood method on the RAxML online platform with 100 bootstrap replicates. The *RcGST* genes were mapped onto chromosomes based on the genome annotation document using TBtools, and tandemly duplicated genes were identified based on previous studies[65,66]. An intraspecies collinearity analysis of *R. chinensis* was conducted to identify segmentally duplicated genes. To study the evolution of GST genes among different plants, collinearity relationships were analyzed to infer the interspecies orthology between *R. chinensis* and other plants using TBtools software. Whole-genome sequences and annotation documents of peach, strawberry, and pear (*Pyrus communis*) were downloaded from the Genome Database for Rosaceae[67]. Whole-genome sequences and annotation documents of apple (*Malus × domestica* 'Golden Delicious') were downloaded from the official website[68]. Whole-genome sequences and annotation documents of grapevine, soybean (*Glycine max*), *Medicago truncatula*, and *Populus trichocarpa* were downloaded from the Ensembl website. An evolutionary tree between species was generated using the LifeMap website[69].

RNA-seq analysis

Twenty-one RNA-Seq libraries were generated from seven samples (S3, D1, D2, D3, D4, PT, and DT), and raw sequence data were deposited in the Genome Sequence Archive at the National Genomics Data Center, China National Center for Bioinformation/Beijing Institute of Genomics, Chinese Academy of Sciences (GSA: CRA006521)[65]. Fragments per kilobase million (FPKM) were used to determine gene expression.

PacBio Iso-Seq long-read sequencing

For PacBio Iso-Seq, full-length cDNA from D2 samples was constructed according to the method described by Liu et al[70]. The amplified cDNA products were built into SMRTbell template libraries in accordance with the IsoSeq protocol (PacBio). The SMRTbell template was then annealed to the sequencing primer and bound to the polymerase. Finally, the templates were sequenced on the PacBio platform by Biomarker Technologies (Biomarker Technologies, Beijing, China). SMRTlink v10.0 software was used for Iso-Seq data analysis. The open

reading frames were detected using TransDecoder v5.0 for isoform sequences to obtain coding and untranslated region sequences.

Quantitative real-time PCR (RT-qPCR) analysis

Total RNA was isolated from different rose samples using an OmniPlant RNA Kit (DNase I) (CoWin Biosciences, Taizhou, China). cDNA was synthesized by reverse transcription from 15 μL of total RNA using the MonScript™ RTIII All-in-One Mix with dsDNase (Monad Biotechnology Co., Ltd, Wuhan, China). *RhUBI2* (JK618216) was used as an internal control[71]. The primers used for real-time PCR are listed in Supplemental Table S3. Real-time PCR was performed as previously described[65].

Statistical analysis

Significant differences ($p < 0.05$) were determined using Student's *t*-test and one-way analysis of variance (ANOVA) tests. The *t*-test was performed using Microsoft Excel 2019 (Seattle, Washington, USA), and ANOVA was conducted using SPSS 23 (SPSS Inc., Chicago, IL, USA). Differential expression analysis between rose samples was performed using DeSeq2 in the OmicShare tool, with a Q-value threshold of 0.05. Venn diagrams were plotted using InteractiVenn[72]. A protein–protein interaction network was generated using the STRING database[73]. Correlation analysis was performed using the corrplot package[74].

Results

Environmental factors affecting color transition in butterfly rose

In the natural environment, the petals of butterfly rose were light yellow at the bud stage (S3) and newly opened flowering stage (D1), turning pink on the second day of flowering (D2) then dark pink at the late flowering stage (D3 and D4) (Fig. 1a). The total anthocyanin content was low at S3 and D1 then increased significantly at D2 and later stages (D3 and D4), resulting in a color change from light yellow to pink and dark pink (Fig. 1b).

The butterfly rose petals turned light pink in the afternoon on the first day of anthesis (D1.5) and the total anthocyanin content of D1.5 samples was slightly higher than that of D1 samples. When D1.5 flowers were subjected to dark conditions until 08:00–09:00 the next day, the petals of D1.5–2 samples were pink and similar in color to those of D2 samples, but with a slightly lower total anthocyanin content (Fig. 1b). This may be because the D1.5–2 samples lacked 3–4 h of evening and morning sunlight. Thus, dark conditions (approximately 15 hours) had little effect on anthocyanin transport.

Treatments with different light intensities were used to study the effect of sunlight on flower color transition. Under PT, the petals of butterfly rose turned pink, similar to those of D2 samples under natural light conditions (Fig. 1a). Under DT, the petals turned almost white on the second day of anthesis. When DT flowers were exposed to natural sunlight for one day, the petal color changed back to pink (Fig. 1a). The total anthocyanin content in PT samples (reduced sunlight) was lower than that in D2 samples under natural light conditions, whereas DT samples (no sunlight) showed low accumulation of total anthocyanins (Fig. 1b). This suggests that sunlight was an important environmental factor influencing PACCs in butterfly rose flowers.
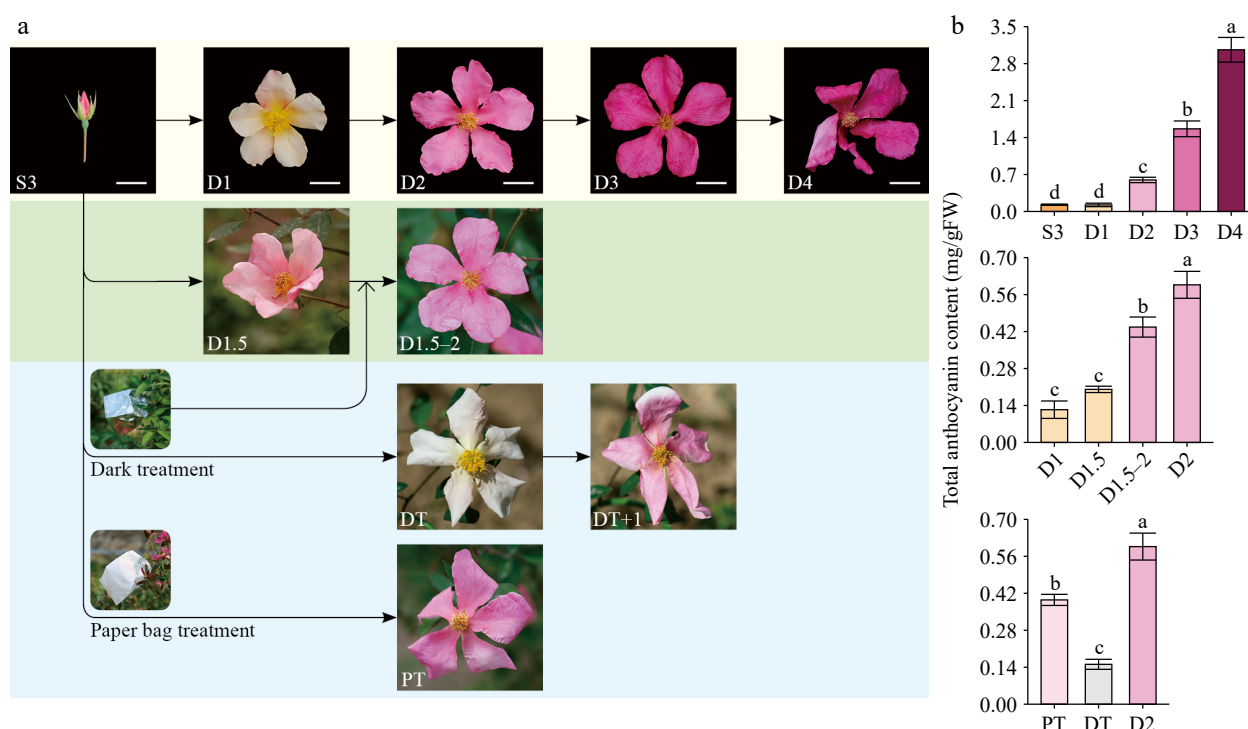
Fig. 1 Phenotypes and total anthocyanins contents of butterfly rose (*R. chinensis* 'Mutabilis') samples. (a) Photos of butterfly rose flowers under natural conditions and different treatments. Scale bars = 2 cm. S3, bud stage (one day before anthesis); D1, first day of anthesis; D2, second day of anthesis; D3, third day of anthesis; D4, fourth day of anthesis. PT, paper bag treatment, DT, dark treatment; DT+1, dark treatment flower exposed to natural sunlight conditions for one day. D1.5, flowers collected in the afternoon (17:30) on the first day of flowering; D1.5–2, flowers at the D1.5 stage that were dark treated until the next morning. (b) Total anthocyanin contents of different butterfly rose samples (*n* = 3–4). Different lowercase letters indicate statistically significant differences (ANOVA test, *p* < 0.05).

Anthocyanin contents in different samples of butterfly rose

Five butterfly rose samples at different developmental stages and two samples under different treatments were selected for anthocyanin analysis (Fig. 2a). Eight anthocyanins were detected in butterfly rose petals in the seven samples (Fig. 2b). More anthocyanin compounds were detected in dark pink samples (D3 and D4). Among the five developmental stages, the contents of five anthocyanins differed significantly between pink and light-yellow samples. Notably, Cy3G had the highest content in all pink samples, accounting for 72% of the total anthocyanin content at D2 and 86% at D4. Cy3G5G had the second-highest anthocyanin content. The other three differentially accumulated anthocyanins had very low contents (< 0.03 mg/gFW in D2 samples). Among the treated and control samples, five anthocyanins were differentially accumulated between DT and sunlight exposure (D2 and PT) samples, including the two main compounds, Cy3G and Cy3G5G (Fig. 2c). Therefore, the change in petal color from light yellow to pink in butterfly rose was caused by the accumulation of high anthocyanin contents, with Cy3G and Cy3G5G being the main components involved in petal coloration.

Structural genes involved in the anthocyanin biosynthetic pathway

Anthocyanins are biosynthesized *via* the flavonoid/anthocyanin biosynthetic pathway, and most structural genes involved in this pathway have been identified (Fig. 3a, Supplemental

Table S1). Samples collected at different developmental stages (S3, D1, and D2) and under different treatments (D2, PT, and DT) were selected for further analyses. The expression patterns of structural genes involved in the anthocyanin biosynthetic pathway (except for UGT genes) in the different samples differed from those of key accumulated anthocyanins (Fig. 3b). Among the 217 candidate UGT genes obtained from the preliminary screening, only 91 were expressed in these five samples (average FPKM ≥ 1). Cluster analysis (Pearson correlation) was performed on the expression patterns of the 91 UGT genes and the contents of key anthocyanins (Fig. 3c). Thirteen UGT genes showed high expression in pink samples and low expression in bud and DT samples. However, only one of these genes had a high expression level, whereas the rest had relatively low expression levels (Fig. 3d). This gene is homologous to *RhUF3GT1*(AB292796)[10] and *UF3GT* (AB239786, partial)[75] and was named *RcUF3GT1*. *RhUF3GT1* and *UF3GT* were cloned from the *R. hybrida* 'Ehigasa' and *R. hybrida* 'Charleston', respectively, both of which are PACC cultivars, and recombinant RhUF3GT1 expressed in yeast can catalyze the 3-glucosylation of anthocyanidins but not flavonols[10]. In butterfly rose the expression pattern of *RcUF3GT1* corresponded to the increase in Cy3G content and RcUF3GT1 encodes a 466 amino acid protein in the D2 sample that shares 97.86% identity with the RhUF3GT1 protein (Supplemental Table S4), indicating that they have the same function. Therefore, among the structural genes involved in the anthocyanin biosynthesis pathway, only *RcUF3GT1* may be involved in PACC.
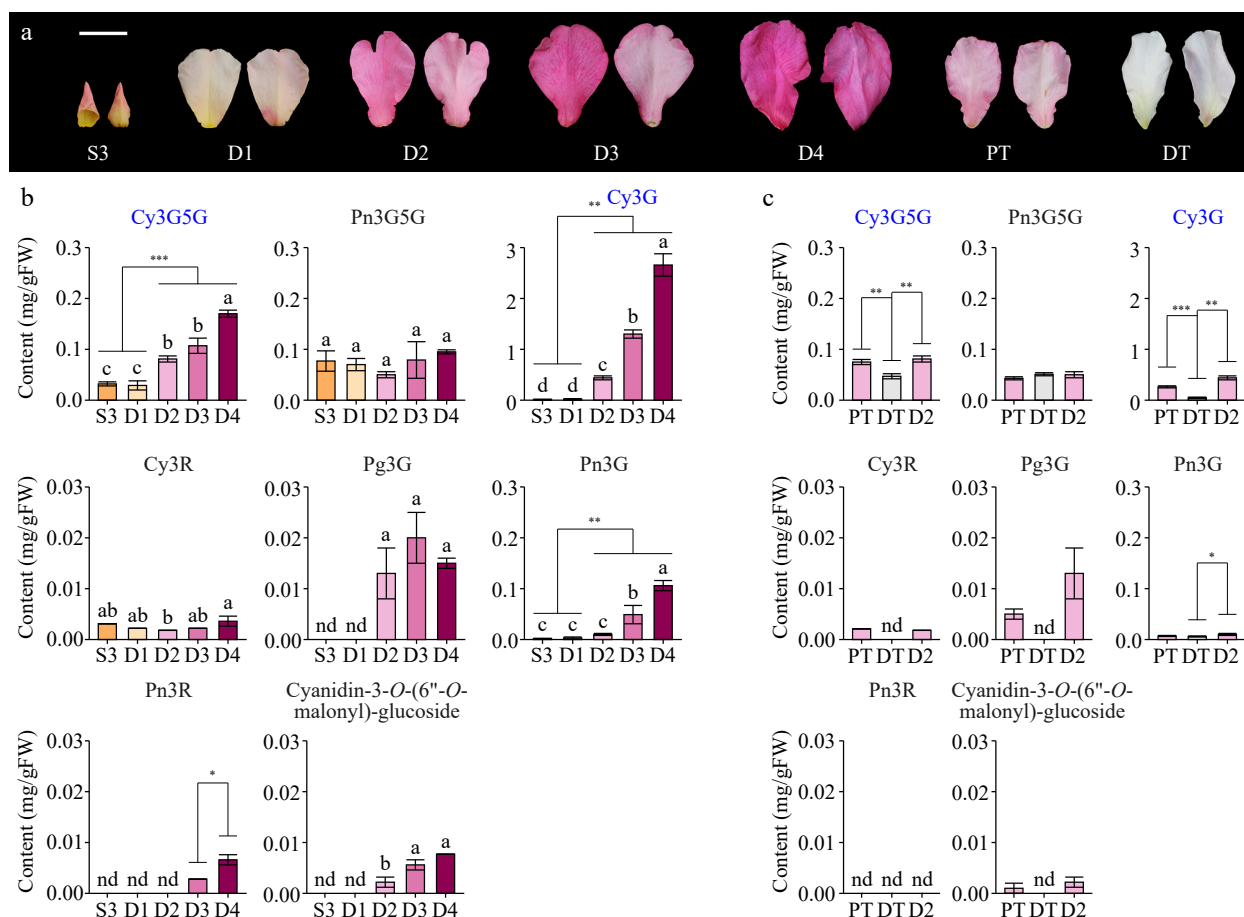
Fig. 2   Anthocyanin compositions in different butterfly rose samples. (a) Adaxial and abaxial surfaces of the petals are shown. Scale bar = 2 cm. (b) Anthocyanin contents of butterfly rose petals at different stages. (c) Anthocyanin contents of butterfly rose petals under different treatments. Data are presented as the mean ± standard error (*n* = 3–4). Pn3R, peonidin-3-*O*-rutinoside; Cy3R, cyanidin-3-*O*-rutinoside. Key anthocyanins are highlighted in blue. Different lowercase letters indicate statistically significant differences (ANOVA test, $p < 0.05$). nd, not detected. *$p < 0.05$, **$p < 0.01$, ***$p < 0.001$ by Student's *t*-test.

Anthocyanin transport genes involved in post-anthesis color change

Identification and analysis of RcGST genes

In total, 80 full-length and 32 partial *RcGST* genes were identified (Supplemental Table S5). To explore the evolutionary relationships between *RcGSTs*, a maximum likelihood phylogenetic tree was constructed using 80 full-length RcGST proteins and 65 AtGST proteins (Fig. 4a). The RcGST family was divided into 12 classes: Tau (U), Phi (F), Lambda (L), Zeta (Z), Theta (T), tetra-chlorohydroquinone dehalogenaselike (TCHQD), dehydroascorbate reductase (DHAR), γ-subunit of the eukaryotic translation elongation factor 1B (EF1Bγ), glutathionyl hydroquinone reductase (GHR), microsomal prostaglandin E synthase type 2 (mPGES-2), GSTs with two thioredoxins (GST2N), and MAPEG[61,76]. The GSTU class was the largest subfamily, with 50 full-length *RcGST* members, followed by the GSTF class, with seven. The other classes had fewer full-length *RcGSTs*, with no more than four in each class. Unlike Arabidopsis, no hemerythrin (GSTH) genes were detected in the rose genome. In addition, GST genes belonging to the metaxin class in the rose genome were incomplete (partial). Identified GST genes were renamed based on their subfamilies and chromosomal locations.

The mapping of 80 full-length and 32 partial *RcGST* genes to the chromosomes of *R. chinensis* revealed an uneven distribution among the chromosomes (Fig. 4b). RcChr 7 contained the largest number of GST genes, with 23 full-length and 13 partial *RcGST* genes, whereas only one *RcGST* gene was located in RcChr 2. Nineteen tandemly duplicated genes were detected in the *R. chinensis* genome, including 13 GSTU, two GSTL, two GSTZ, and two MAPEG genes. Additionally, six segmentally duplicated GST genes were detected, including five GSTU genes and one GSTL gene. These *RcGST* genes formed 12 gene clusters, including seven clusters comprising GSTU genes and one cluster comprising GSTU and GSTL genes. This indicates that the expansion of the GST gene family in *R. chinensis* was driven by tandem and segmental duplication, particularly in the GSTU and GSTL classes.

RcGST(s) involved in anthocyanin transport

Previous studies have shown a positive correlation between anthocyanin content and the expression of GST genes involved in anthocyanin transport[33,77]. To screen for GSTs involved in anthocyanin transport, we excluded genes with low expression levels (average FPKM < 1 in the five samples). A total of 42 full-length GST genes and five partial GST genes were expressed in these samples. Correlation analysis between gene expression levels and key anthocyanin contents showed that only *RcGSTF2* and *RcGSTU39* exhibited high correlation coefficients (Pearson $r \geq 0.80$) with the two key anthocyanins (Fig. 5a). Analysis of the
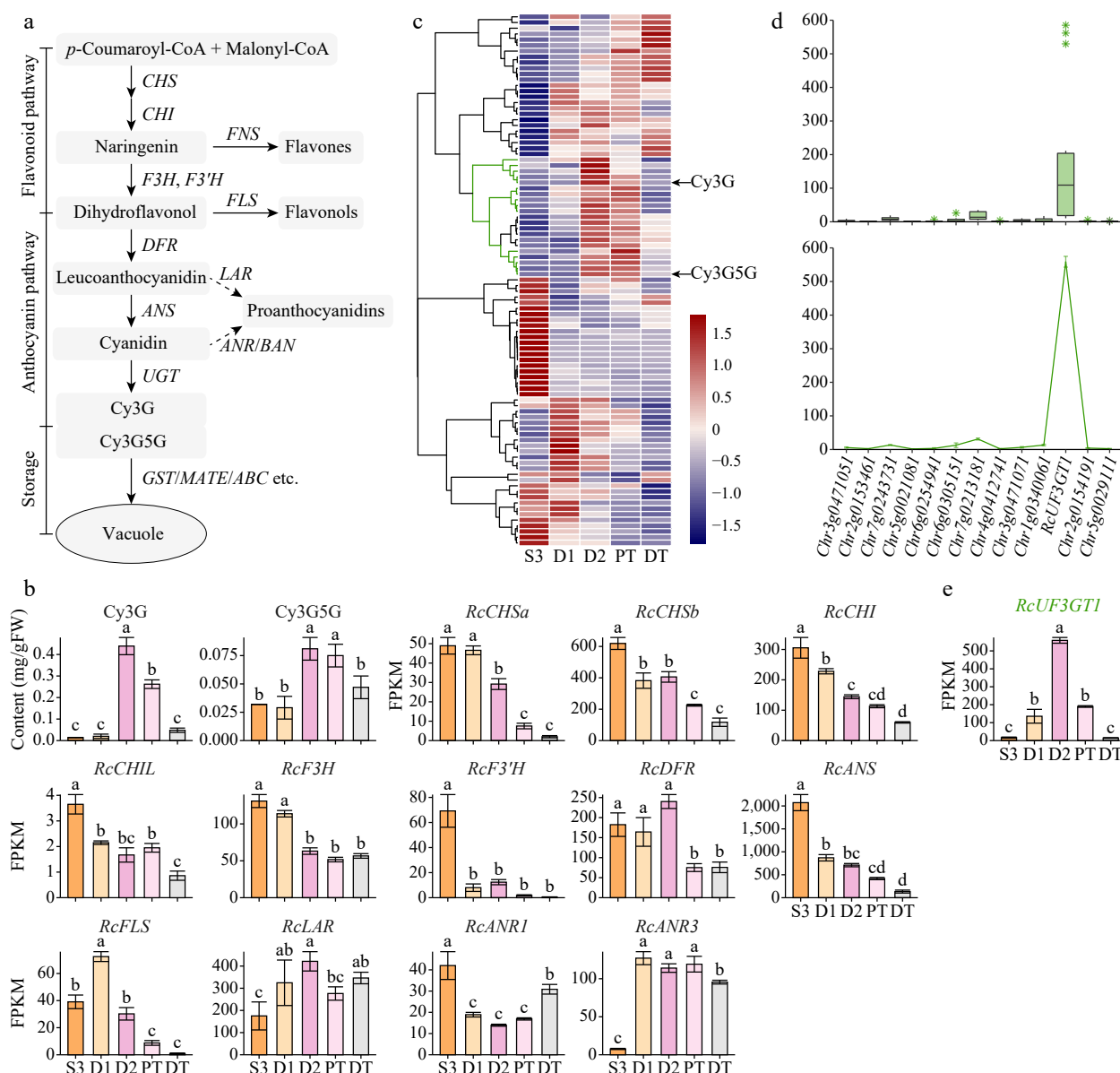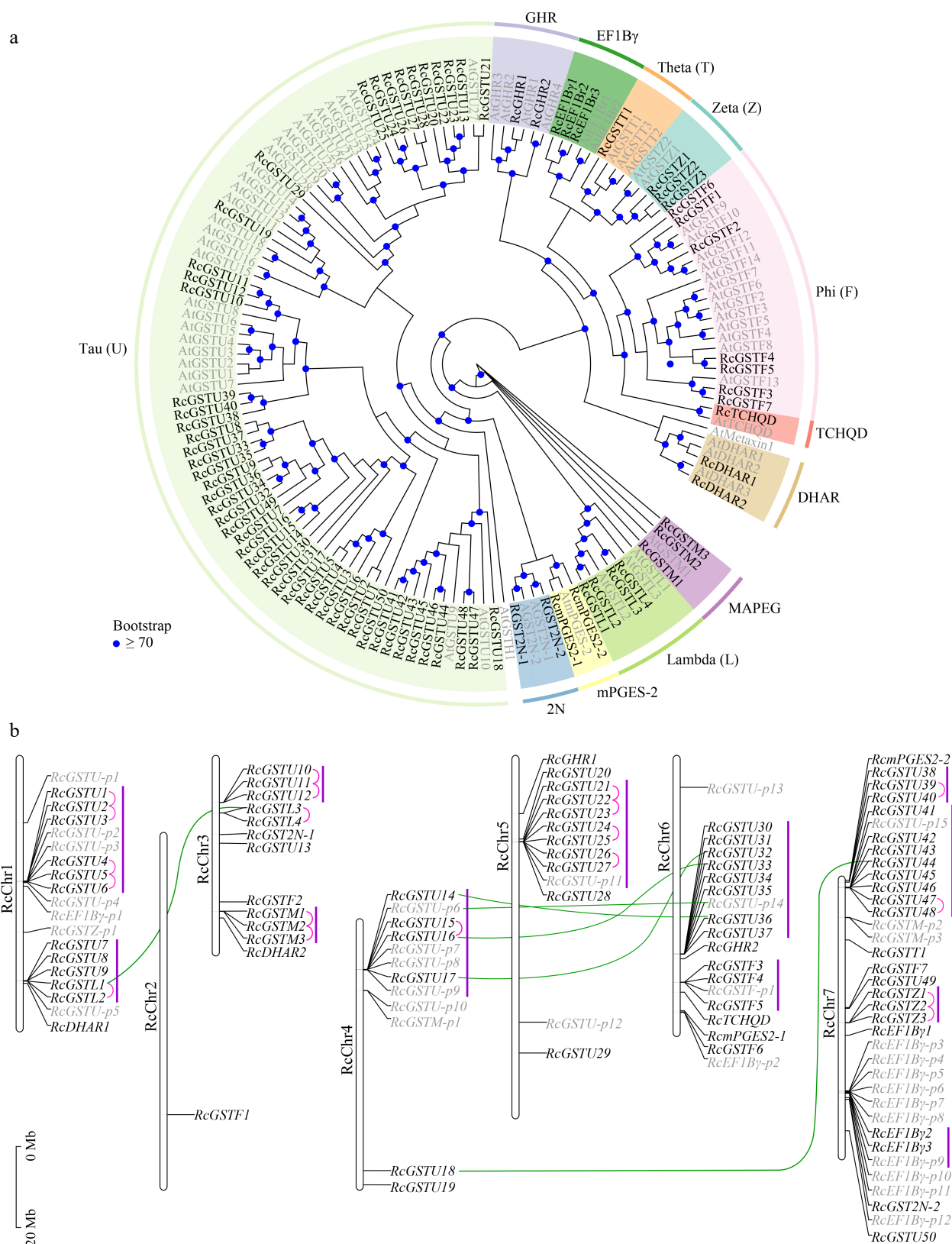
Fig. 3 Expression patterns of structural genes involved in the anthocyanin biosynthetic pathway. Data are presented as the mean ± standard error (*n* = 3). Different lowercase letters indicate statistically significant differences (ANOVA test, *p* < 0.05). (a) Schematic representation of the anthocyanin biosynthetic pathway in plant cells[23]. CHS, chalcone synthase; CHI, chalcone isomerase; FNS, flavone synthase; F3H, flavanone 3-hydroxylase; F3'H, flavonoid 3'-hydroxylase; FLS, flavonol synthase; DFR, dihydroflavonol reductase; ANS, anthocyanidin synthase; UGT, UDP-glycosyltransferase; LAR, leucoanthocyanidin reductase; ANR, anthocyanidin reductase; BAN, BANYULS. (b) Expression profiles of two key anthocyanins and structural genes in anthocyanin biosynthetic pathway (excluding UGT genes). (c) Clustering heatmap of UGT genes expressed in petals (Pearson correlation, clustering_method = 'complete'). (d) Expression levels of candidate UGT genes. Boxplot, average expression levels in five samples; line plot, expression levels in D2 samples. *RcUF3GT1*, RchiOBHmChr1g0383951. (e) Expression patterns of *RcUF3GT1* in five samples.

expression patterns indicated that only *RcGSTF2* expression was consistent with the accumulation of key anthocyanins, particularly Cy3G (Fig. 5b). The amino acid sequences of 80 full-length *RcGSTs* were aligned with those of other functionally identified GST proteins using MAFFT software, and a neighbor-joining evolutionary tree was constructed using MEGA7.0 software (Fig. 5c). Phylogenetic analysis revealed that only RcGSTF2 clustered with the characterized GSTs involved in anthocyanin transport in other plants, especially other Rosaceae plants, indicating their functional similarity. These results indicated

that *RcGSTF2* is the only candidate GST gene involved in anthocyanin transport. To investigate the evolutionary relationship of GST genes involved in anthocyanin transport across different plants, rose and four other Rosaceae plants (peach, apple, pear, strawberry), two Fabaceae plants (*Medicago truncatula* and soybean), and one Salicaceae plant (*Populus trichocarpa*) were selected for inter-species collinearity analysis. These eight plants belong to the fabids of Rosales, with grapevine (belonging to Vitales) selected as the outgroup of the evolutionary tree. The results showed that GST genes involved in
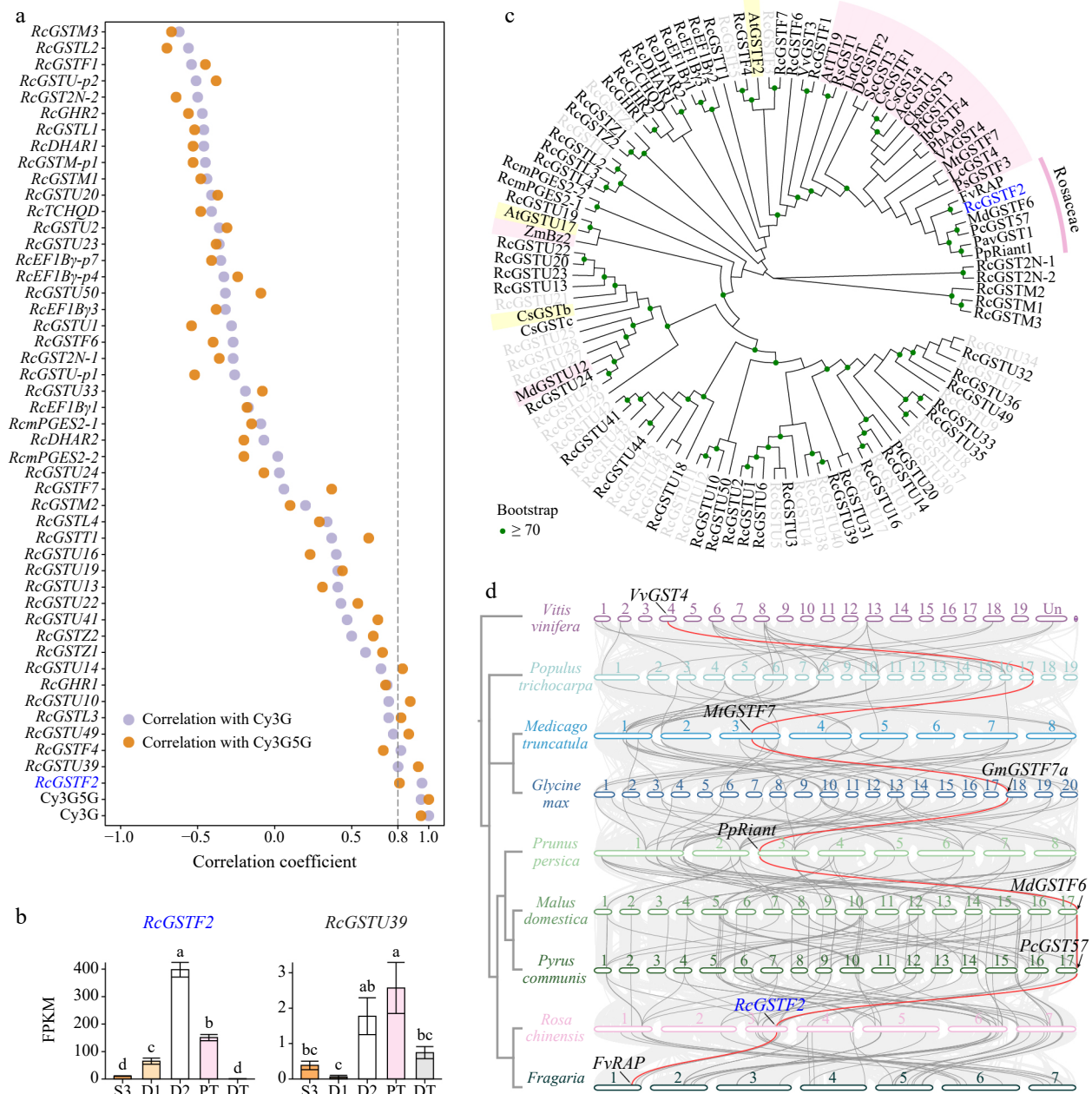
Fig. 4 Identification and analysis of GSTs in the *R. chinensis* genome. (a) Maximum likelihood phylogenetic analysis and classification of putative full-length RcGST genes. Genome IDs of AtGSTs (shown in gray) are listed in Supplemental Table S2. (b) Chromosomal distribution of full-length and partial RcGST genes. Full-length GST genes are represented by black letters; putative partial GST (GST-p) genes are represented by gray letters. Pink lines indicate tandemly duplicated genes; green lines indicate segmentally duplicated genes. Gene clusters are indicated by purple lines.

Fig. 5 GST(s) involved in anthocyanin transport. (a) Pearson correlation coefficient between petal-expressed *RcGSTs* and two key anthocyanins in five samples. (b) Expression profiles of two key anthocyanins and two candidate *RcGSTs* in different samples. Data are presented as the mean ± standard error ($n = 3$). Different lowercase letters indicate statistically significant differences (ANOVA test, $p < 0.05$). (c) Neighbor-joining phylogenetic tree of full-length RcGSTs and other characterized GST proteins. Encoding proteins of the *RcGSTs* that were not expressed in butterfly rose petals are represented by gray letters. GSTs involved in anthocyanin transport and flavonoid transport are highlighted with pink and yellow backgrounds, respectively. GST sequences used in this analysis are listed in Supplemental Table S6. (d) Inter-species collinearity analysis among eight fabid plants and grapevine. Collinear blocks are represented by light gray lines in the background; collinear GST genes are represented by gray lines; collinear genes of *RcGSTF2* are highlighted in red. GSTs characterized in these species were labeled as follows: *VvGST4*, NP_001267869.1 (VIT_13s0067g03420); *MtGSTF7*, Medtr3g064700[35]; *GmGSTF7a*, Glyma.18G043700[35]; *PpRiant* (*PpGST1*), Prupe.3G013600[28,29]; *MdGSTF6*, MD17G1272100[22]; *PcGST57*, pycom17g27080[78]; *FvRAP*, FvH4_1g27460[32].

anthocyanin transport exhibited collinearity across these plants, indicating conserved evolution (Fig. 5d)[77]. The bioinformatics analysis showed that *RcGSTF2* may be involved in the anthocyanin transport in butterfly rose.

Other genes involved in anthocyanin transport

BLASTp analysis (pident ≥ 55%, E-value < 1e−50) identified nine orthologs of *AtABCC2/VvABCC1/ZmMRP3/OsMRP15* in the

rose genome. In addition, three orthologs of *AtTT12/CaMATE1* (pident ≥ 70%, E-value < 1e−50) and seven orthologs of *SlMTP77/MtMATE2/VvAM1/VvAM3* (pident ≥ 55%, E-value < 1e−50) were detected in the rose genome (Supplemental Table S7). Of these 19 orthologs, eight genes were petal-expressed (average FPKM in five samples ≥ 1). Most genes exhibited low correlation coefficients with Cy3G or Cy3G5G and only *RcABCC2b* exhibited a

trend similar to that of anthocyanin accumulation (Fig. 6). However, only four partial transcripts of *RcABCC2b* were detected in D2 samples, and the identity of the longest protein sequence encoded by them and the corresponding genome protein sequence was 33.73% (Supplemental Table S4). Whether *RcABCC2b* was involved in the transport of anthocyanins in butterfly roses is not clear.

Other differentially expressed genes involved in post-anthesis color change

To identify other genes involved in the flower color change of butterfly rose, the following criteria were applied: (1) upregulated expression (Log$_2$FC ≥ 1, Q < 0.05) in color-changing petals (D2) compared to bud (S3) samples, and (2) upregulated expression in pink samples (D2 and PT) compared to white samples (DT) (Fig. 7a). Venn analysis of the number of differentially expressed genes (DEGs) between different samples revealed that 754 genes were co-upregulated (Fig. 7b). Considering that the biosynthesis of anthocyanins in the D1 stage has just started, we calculated the correlation coefficients between the expression levels of these 754 candidate DEGs and the accumulation of key anthocyanins (Cy3G and Cy3G5G) for four samples (S3, D2, PT, and DT). Genes with higher expression levels (average FPKM ≥ 2 in four samples) and higher correlation coefficients (Pearson r ≥ 0.80) with both key anthocyanins (Fig. 7c) were selected.

A total of 445 DEGs were identified, including *RcPAL2*, 12 *UGTs*, *RcGSTF2*, and *RcABCC2b*. Among these, four R2R3-MYB genes (*RcMYB1*, *RcMYB114a*, *RcMYB41*, and *RcMYB106L*), four WD40 genes (*RcSPA1*, *RcRUP1*, *RcCOP1L*, and *RcSPA3*), three BBX genes (*RcBBX28*, *RcBBX31*, and *RcBBX32*), four bZIP genes (including *RcHYH* and *RcHY5*), three NAC genes, and four WRKY genes were identified as DEGs. No differentially expressed bHLH genes were detected. Key DEGs and their genome IDs are listed in Supplemental Table S8.

The protein sequences of the four differentially expressed R2R3-MYB genes, along with those of other R2R3-MYB protein sequences involved in anthocyanin biosynthesis, were used to construct a neighbor-joining phylogenetic tree (Fig. 7d). Among these, *RcMYB41* and *RcMYB106L* belong to subgroup 9 and potentially involved in epidermal cell outgrowth[79]. *RcMYB1* and *RcMYB114a* were clustered with MYBs that

activate anthocyanin accumulation in other plants (subgroup 6) and positively regulate anthocyanin biosynthesis[17,18,80].

To predict the potential functions and relationships of these genes, we constructed a protein–protein interaction network among the DEGs involved in anthocyanin-related pathways. The results indicate that some BBX, bZIP, NAC, and WKRY transcription factors might be involved in PACC, while *RcHY5*, *RcCOP1L* and *RcHYH* might be the core regulators of color transition in rose petals. Indeed, *RhHY5* induced the expression of *RhMYB114a* under light conditions in 'Burgundy Iceberg' rose[17]. However, the regulatory network of *RcMYB114a*, *RcGSTF2* and *RcUF3GT1* remain unclear.

Analysis of candidate genes

Based on the above analysis, 21 candidate DEGs including four structural genes (*RcUF3GT1*, *RcGSTF2*, *RcABCC2b*, and *RcPAL2*) and 17 transcription factors were selected for further analysis (Supplemental Table S4). The genes whose transcripts encoding protein sequences showed high identity (> 60%) with corresponding genome protein were selected for RT-qPCR analysis. The expression levels of 15 candidate genes were analyzed in butterfly rose and *R. hybrida* 'Spectra'), both of which were PACC cultivars (Fig. 8a). In *R. hybrida* 'Spectra' petals, no anthocyanins were detected in the yellow petal (pre-change, SY) samples, whereas more anthocyanins accumulated in the red petal (post-change, SR) samples (Fig. 8b & c). The main anthocyanins that accumulated in the SR samples were Pg3G (76.84%) and Pg3G5G (12.14%), which differed from the anthocyanin profiles of D2 samples.

In butterfly rose samples, RT-qPCR analysis confirmed the expression patterns of *RcUF3GT1* and *RcGSTF2*, whose expression showed high correlations with anthocyanin contents, while the expression of *RcPAL2* and *RcABCC2b* showed low correlations with anthocyanin contents. Similarly, *RcUF3GT1* and *RcGSTF2* were expressed higher in SR samples than in SY samples (Fig. 8d). In addition, RT-qPCR and correlation analysis on candidate transcription factors showed that *RcMYB114a* and *RcBBX28* showed high correlations with anthocyanin contents in butterfly rose and were differentially expressed in *R. hybrida* 'Spectra' petals (Fig. 8d & e, Supplemental Fig. S3). Two distinct alternative splicing variants of *RcHYH* were detected in D2 samples (Supplemental Table S4), and the expression of
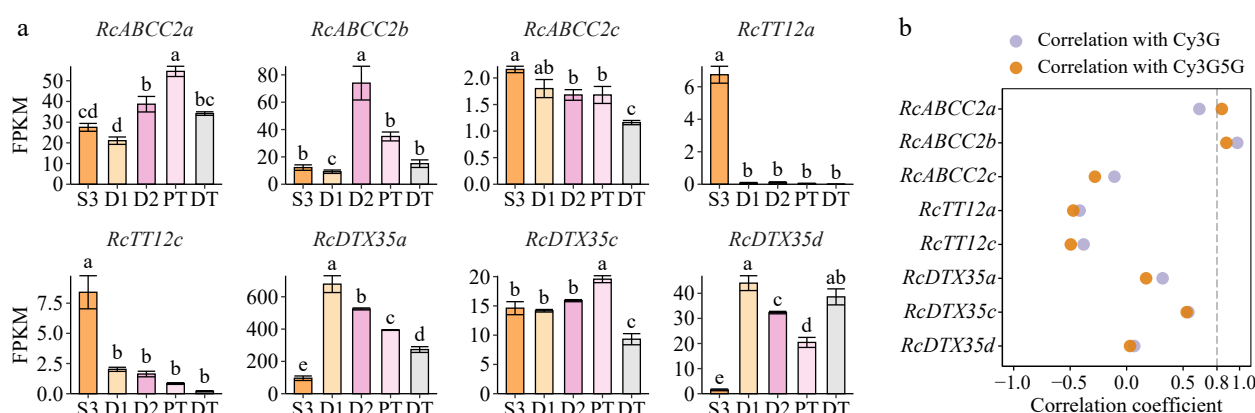

Fig. 6 Orthologs of anthocyanin-related MATE and ABCC transporters in butterfly rose petals. Their genome IDs are listed in Supplemental Table S7. (a) Expression patterns of ABC and MATE genes in different samples of butterfly rose. Data are presented as the mean ± standard error (*n* = 3). Different lowercase letters indicate statistically significant differences (ANOVA test, *p* < 0.05). (b) Pearson correlation coefficient between candidate genes and two key anthocyanins in five samples.
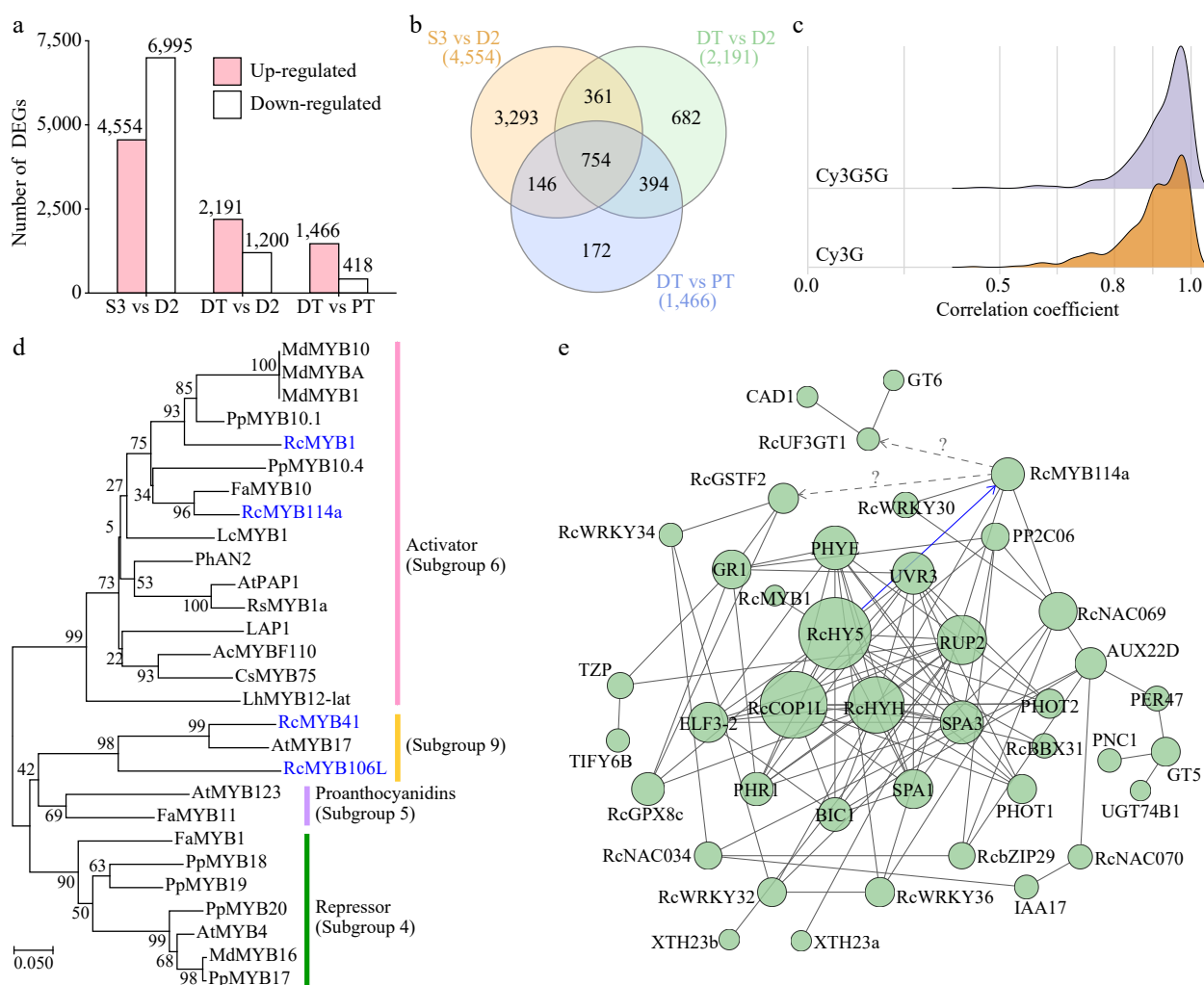
Fig. 7 Differentially expressed genes (DEGs) during the post-anthesis color transition. (a) Number of DEGs between different samples. (b) Venn analysis of the number of DEGs. (c) Correlation coefficients between DEGs (average FPKM ≥ 2 in four samples) and key anthocyanins. (d) Neighbor-joining phylogenetic tree of four candidate R2R3-MYB proteins (highlighted in blue) with other characterized R2R3-MYBs. Protein sequences used in this analysis are listed in Supplemental Table S9. (e) Protein–protein interaction network of DEGs (confidence = 0.20). Their genome IDs are listed in Supplemental Table S10. The identified interaction is displayed as a blue line.

RcHYH-X1 and *RcHYH-X2* were more sensitive to sunlight than *RcHY5*. The expression patterns of *RcHY5*, *RcHYH*, and *RcCOP1L* were not strongly correlated with the anthocyanin content in different rose samples and their functions require further research. Together, these results suggest that *RcUF3GT1*, *RcGSTF2*, *RcMYB114a* and *RcBBX28* are crucial genes involved in the post-anthesis transition in rose petals.

Discussion

Flower color is a signal that plants use to communicate with their visitors; different messages can be sent to visitors by changing flower color. The retention of old flowers favors the attraction of visitors over long distances and directs nearby visitors toward rewarding flowers[3]. In this study, it was observed that visitors of butterfly rose flowers, including hoverflies and Italian bees, preferentially visited pre-changed (D1) flowers, followed by slightly post-changed (D2) flowers. White flowers after dark treatment were also popular among visitors. Hoverflies and bees preferred UV-absorbing yellow colors, which may contain pigments such as flavonoids and aurane chalcones[81]. From the bees' perspective, red appears similar to the background color of green leaves[3]. Therefore, plants such as butterfly rose change their flower color by accumulating anthocyanins in their petals to form different visual signals for visitors. This is a color-changing strategy used by many natural bee-pollinated plants[82].

PACCs in different plants are induced by different structural genes. The transition of flower color from acyanic (white and yellow) to cyanic (pink, red, and purple) is primarily due to an increase in anthocyanin content, accompanied by the upregulation of structural genes involved in the anthocyanin biosynthesis pathway[8,46,83]. In *Viola cornuta*, *VcANS* is the key regulated gene for floral color change during development, whereas the upregulated expression of *NmCHS* is associated with an increase in anthocyanin content in *Nicotiana mutabilis* petals[8,9]. In *Pleroma raddianum*, *CHS* and *ANS* are upregulated during color transition[84]. In the present study, among the structural genes involved in the flavonoid/anthocyanin biosynthetic pathway, only *RcUF3GT1*, and several other low-expression
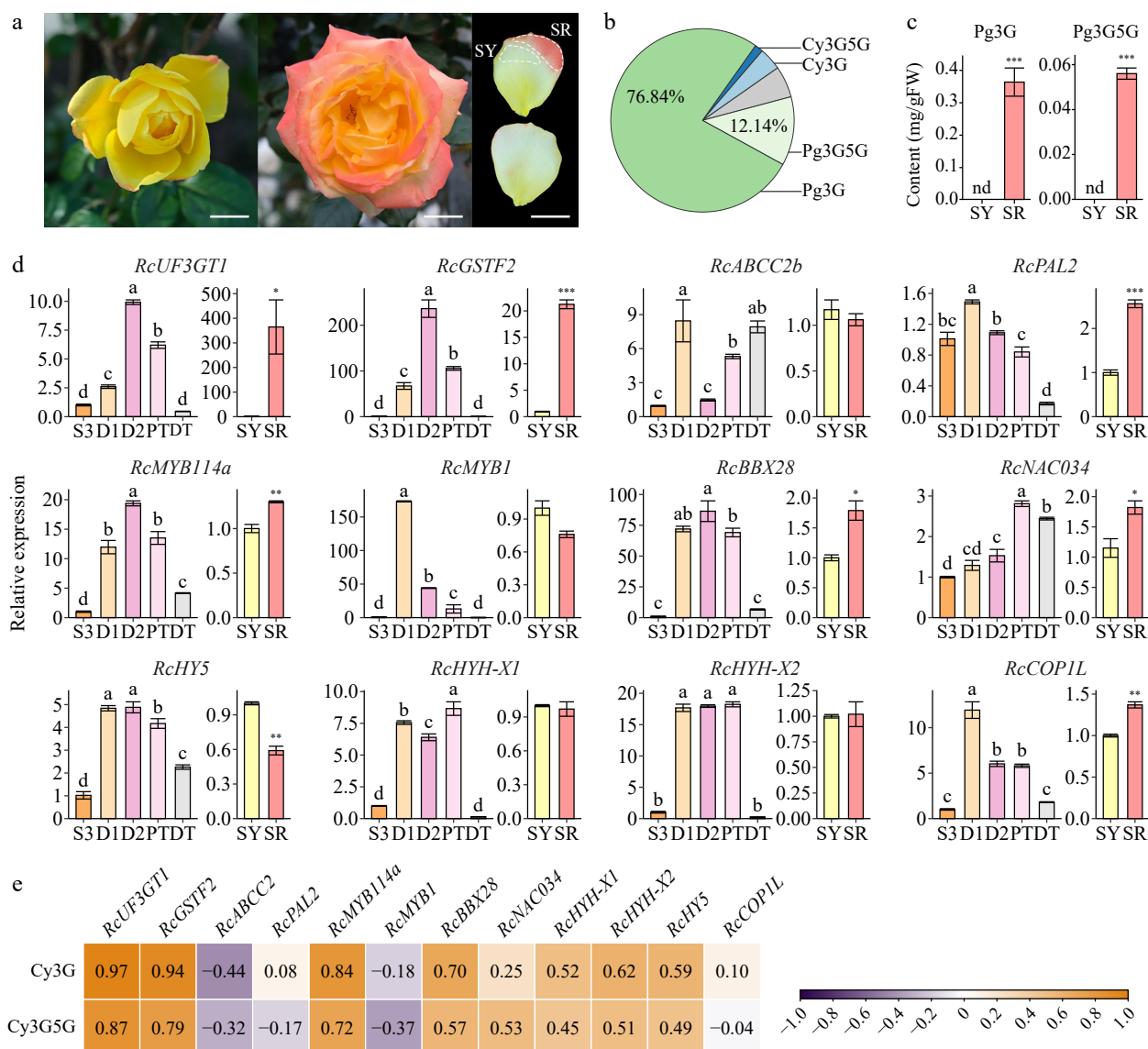
Fig. 8 Analysis of candidate DEGs. Data are presented as the mean ± standard error ($n = 3$). (a) Photos of *R. hybrida* 'Spectra'. Scale bars = 2 cm. Left, newly opened flower; middle, full-bloom flower (fourth or fifth day of anthesis); upper right, adaxial surface of collected petal; lower right, abaxial surface of collected petal. (b) Two key anthocyanin contents in different samples of *R. hybrida* 'Spectra'. (c) Anthocyanin components in the red part of middle-layer petals of *R. hybrida* 'Spectra' (SR). (d) Expression levels of candidate DEGs in different samples of *R. chinensis* (ANOVA test, $p < 0.05$). and *R. hybrida* 'Spectra' (Student's *t*-test, *$p < 0.05$, **$p < 0.01$). (e) Correlation analysis between the expression of candidate DEGs and key anthocyanins in butterfly rose samples.

UGT genes showed similar expression patterns for anthocyanin accumulation in petals, similar to that in safflower (*Carthamus tinctorius*)[52]. Among previous studies on PACC rose cultivars, such as 'Charleston', 'Ehigasa', and 'Masquerade', all cultivars accumulate Cy3G and Cy3G5G in the post-change petals[45,46], which was the same for butterfly rose. Different anthocyanin profiles accumulated in the post-change petals of *R. hybrida* 'Spectra', mainly Pg3G and Pg3G5G (Fig. 8b). This suggests that anthocyanins causing the color change in rose were not limited to cyanidin glycosides. Therefore, we speculate that the glycosylation of anthocyanidin is regulated during the post-anthesis color transition in rose flowers.

Many rose cultivars are self-incompatible, such as *R. chinensis* var. *spontanea* and *R. chinensis* 'Slater's Crimson China'[85,86]. Under semi-transparent PT conditions, the exclusion of foreign pollen still resulted in a color change (Fig. 1a). This indicates that pollination may not be a key factor affecting PACC in butterfly rose. The same phenomenon was observed in *Weigela japonica* var. *sinica*, and its color change was independent of pollinator visits and flower pollination[2]. In the present study, a positive correlation was observed between anthocyanin accumulation and light intensity at the D2 stage. Butterfly rose petals showed minimal accumulation of anthocyanins under dark treatment but continued to accumulate anthocyanins after exposure to sunlight (Fig. 1a). It indicates that light is an important environmental factor affecting anthocyanin production.

In this study many differentially expressed transcription factors are involved in the light signaling pathway (Supplemental Table S10). As a major positive regulator of light signaling in

plants, HY5 directly binds to the promoters of anthocyanin biosynthesis genes and MYB transcription factors to regulate anthocyanin synthesis[87,88]. A recent study on rose flowers showed that *RhHY5* induces the expression of *RhMYB114a* and positively regulates anthocyanin biosynthesis by directly activating anthocyanin structural genes *via* the MYB114a-bHLH3-WD40 complex[17]. R2R3-MYBs can directly regulate structural genes involved in the anthocyanin biosynthesis, as well as GST transporter of anthocyanins[22,29]. Whether *RcMYB114a* can directly regulate *RcUF3GT1* and *RcGSTF2* requires further experimental verification. HYH also regulates anthocyanin accumulation in pear and peach[89,90]. In pear fruits, *PybZIPa* promotes anthocyanin biosynthesis by regulating *PyMYB114*, *PyMYB10*, *PyBBX22* and *PyUFGT*[89]. In peach fruit, *PpHYH* activates *PpMYB10* in the presence of the cofactor *PpBBX4*, leading to anthocyanin accumulation in sun-exposed peels[90]. *PavBBX6* and *PavBBX9* can positively regulate light-induced anthocyanin in *Prunus avium* by promoting *PavUFGT*, while the PpBBX16/PpHY5 complex strongly induced the promoter activity of *PpMYB10* in *Pyrus pyrifolia*[19,91]. BBX28 negatively regulate flowering in Arabidopsis, and the PIF8-BBX28 module regulates petal senescence in rose flowers[49,92]. RcCOP1L does not interact physically with RcHY5, and its function is unknown[54]. Further research is required to elucidate the complex regulatory network involved in light-induced anthocyanin pigmentation in *R. chinensis* 'Mutabilis' flowers.

Conclusions

This study elucidated the mechanisms underlying color transitions in rose flowers. We found that color changes in butterfly rose flowers resulted from an increased accumulation of anthocyanins, with Cy3G and Cy3G5G being the key components. Trace amounts of anthocyanins accumulated in the dark-treated samples, whereas pigmentation occurred in the samples exposed to sunlight. Thus, sunlight plays a crucial role in the post-change pink coloration of *R. chinensis* 'Mutabilis'. Among the structural genes involved in the flavonoid/anthocyanin biosynthetic pathway, only *RcUF3GT1* was significantly correlated with anthocyanin accumulation in butterfly rose flowers. Among the 80 genome-wide identified full-length *RcGST* genes, the expression patterns, and bioinformatics analyses highlighted the involvement of *RcGSTF2* in anthocyanin transport. Orthologs of anthocyanin-related MATE and ABCC transporters were inactive in butterfly rose petals. *RcMYB114a* was considered an important positive transcription factor. Additionally, *RcBBX28* might play significant roles in regulating anthocyanin biosynthesis during post-anthesis color change. These insights contribute to our knowledge of flower color change and have implications for further research on plant genetics and flower color evolution.

Author contributions

The authors confirm contribution to the paper as follows: study conception and design: Kong Y, Bai J; sample collection: Kong Y, Qiu L, Dou X, Lang L; laboratory analysis: Kong Y, Wang H; draft manuscript preparation: Kong Y; feedback on the analysis and manuscript: Wang H, Bai J. All authors reviewed the results and approved the final version of the manuscript.

Data availability

The datasets generated during and/or analyzed during the current study are available from the corresponding author on reasonable request.

Acknowledgments

Conflict of interest

The authors declare that they have no conflict of interest.

Dates

References

1. Boehm MMA, Ojeda DI, Cronk QCB. 2017. Dissecting the 'bacon and eggs' phenotype: transcriptomics of post-anthesis colour change in *Lotus*. *Annals of Botany* 120:563−75
2. Zhang Y, Zhao X, Huang S, Zhang L, Zhao J. 2012. Temporal pattern of floral color change and time retention of post-change flowers in *Weigela japonica* var. *sinica* (Caprifoliaceae). *Journal of Systematics and Evolution* 50:519−26
3. Brito VLG, Weynans K, Sazima M, Lunau K. 2015. Trees as huge flowers and flowers as oversized floral guides: the role of floral color change and retention of old flowers in *Tibouchina pulchra*. *Frontiers in Plant Science* 6:362
4. Weiss MR. 1995. Floral color change: a widespread functional convergence. *American Journal of Botany* 82:167−85
5. Monniaux M. 2023. Unusual suspects in flower color evolution. *Science* 379:534−35
6. Xia Y, Chen W, Xiang W, Wang D, Xue B, et al. 2021. Integrated metabolic profiling and transcriptome analysis of pigment accumulation in *Lonicera japonica* flower petals during colour-transition. *BMC Plant Biology* 21:98
7. Amrhein N, Frank G. 1989. Anthocyanin formation in the petals of *Hibiscus mutabilis* L. *Zeitschrift für Naturforschung C* 44:357−60
8. Macnish AJ, Jiang C, Negre-Zakharov F, Reid MS. 2010. Physiological and molecular changes during opening and senescence of *Nicotiana mutabilis* flowers. *Plant Science* 179:267−72
9. Farzad M, Griesbach R, Hammond J, Weiss MR, Elmendorf HG. 2003. Differential expression of three key anthocyanin biosynthetic genes in a color-changing flower, *Viola cornuta* cv. yesterday, today and tomorrow. *Plant Science* 165:1333−42
10. Fukuchi-Mizutani M, Akagi M, Ishiguro K, Katsumoto Y, Fukui Y, et al. 2011. Biochemical and molecular characterization of anthocyanidin/flavonol 3-glucosylation pathways in *Rosa×hybrida*. *Plant Biotechnology* 28:239−44
11. Li M, Sun Y, Lu X, Debnath B, Mitra S, et al. 2019. Proteomics reveal the profiles of color change in *Brunfelsia acuminata* flowers. *International Journal of Molecular Sciences* 20:2000
12. Yan J, Wang M, Zhang L. 2018. Light induces petal color change in *Quisqualis indica* (Combretaceae). *Plant Diversity* 40:28−34

13. McGimpsey VJ, Lord JM. 2015. In a world of white, flower colour matters: a white–purple transition signals lack of reward in an alpine *Euphrasia*. *Austral Ecology* 40:701–08

14. Zhao D, Tao J. 2015. Recent advances on the development and regulation of flower color in ornamental plants. *Frontiers in Plant Science* 6:261

15. Xu W, Dubos C, Lepiniec L. 2015. Transcriptional control of flavonoid biosynthesis by MYB–bHLH–WDR complexes. *Trends in Plant Science* 20:176–85

16. Raymond O, Gouzy J, Just J, Badouin H, Verdenaud M, et al. 2018. The *Rosa* genome provides new insights into the domestication of modern roses. *Nature Genetics* 50:772–77

17. Yan Y, Zhao J, Lin S, Li M, Liu J, et al. 2023. Light-mediated anthocyanin biosynthesis in rose petals involves a balanced regulatory module comprising transcription factors RhHY5, RhMYB114a, and RhMYB3b. *Journal of Experimental Botany* 74:erad253

18. He G, Zhang R, Jiang S, Wang H, Ming F. 2023. The MYB transcription factor RcMYB1 plays a central role in rose anthocyanin biosynthesis. *Horticulture Research* 10: uhad080

19. Wang Y, Xiao Y, Sun Y, Zhang X, Du B, et al. 2023. Two B-box proteins, PavBBX6/9, positively regulate light-induced anthocyanin accumulation in sweet cherry. *Plant Physiology* 192:2030–48

20. Zhang S, Chen Y, Zhao L, Li C, Yu J, et al. 2020. A novel NAC transcription factor, MdNAC42, regulates anthocyanin accumulation in red-fleshed apple by interacting with MdMYB10. *Tree Physiology* 40:413–23

21. Alabd A, Ahmad M, Zhang X, Gao Y, Peng L, et al. 2022. Light-responsive transcription factor PpWRKY44 induces anthocyanin accumulation by regulating *PpMYB10* expression in pear. *Horticulture Research* 9:uhac199

22. Jiang S, Chen M, He N, Chen X, Wang N, et al. 2019. MdGSTF6, activated by MdMYB1, plays an essential role in anthocyanin accumulation in apple. *Horticulture Research* 6:40

23. Kaur S, Sharma N, Kapoor P, Chunduri V, Pandey AK, et al. 2021. Spotlight on the overlapping routes and partners for anthocyanin transport in plants. *Physiologia Plantarum* 171:868–81

24. Marrs KA, Alfenito MR, Lloyd AM, Walbot V. 1995. A glutathione S-transferase involved in vacuolar transfer encoded by the maize gene *Bronze-2*. *Nature* 375:397–400

25. Alfenito MR, Souer E, Goodman CD, Buell R, Mol J, et al. 1998. Functional complementation of anthocyanin sequestration in the vacuole by widely divergent glutathione *S*-transferases. *The Plant Cell* 10:1135–49

26. Sun Y, Li H, Huang J. 2012. *Arabidopsis* TT19 functions as a carrier to transport anthocyanin from the cytosol to tonoplasts. *Molecular Plant* 5:387–400

27. Kitamura S, Akita Y, Ishizaka H, Narumi I, Tanaka A. 2012. Molecular characterization of an anthocyanin-related glutathione *S*-transferase gene in cyclamen. *Journal of Plant Physiology* 169:636–42

28. Cheng J, Liao L, Zhou H, Gu C, Wang L, et al. 2015. A small indel mutation in an anthocyanin transporter causes variegated colouration of peach flowers. *Journal of Experimental Botany* 66:7227–39

29. Zhao Y, Dong W, Zhu Y, Allan AC, Lin-Wang K, et al. 2020. *PpGST1*, an anthocyanin-related glutathione *S*-transferase gene, is essential for fruit coloration in peach. *Plant Biotechnology Journal* 18:1284–95

30. Pérez-Díaz R, Madrid-Espinoza J, Salinas-Cornejo J, González-Villanueva E, Ruiz-Lara S. 2016. Differential roles for VviGST1, VviGST3, and VviGST4 in proanthocyanidin and anthocyanin transport in *Vitis vinífera*. *Frontiers in Plant Science* 7:1166

31. Hu B, Zhao J, Lai B, Qin Y, Wang H, et al. 2016. *LcGST4* is an anthocyanin-related *glutathione S-transferase* gene in *Litchi chinensis* Sonn. *Plant Cell Reports* 35:831–43

32. Luo H, Dai C, Li Y, Feng J, Liu Z, et al. 2018. *Reduced Anthocyanins in Petioles* codes for a GST anthocyanin transporter that is essential for the foliage and fruit coloration in strawberry. *Journal of Experimental Botany* 69:2595–608

33. Wei K, Wang L, Zhang Y, Ruan L, Li H, et al. 2019. A coupled role for *CsMYB75* and *CsGSTF1* in anthocyanin hyperaccumulation in purple tea. *The Plant Journal* 97:825–40

34. Kou M, Liu Y, Li Z, Zhang Y, Tang W, et al. 2019. A novel *glutathione S-transferase* gene from sweetpotato, *IbGSTF4*, is involved in anthocyanin sequestration. *Plant Physiology and Biochemistry* 135:395–403

35. Wang R, Lu N, Liu C, Dixon RA, Wu Q, et al. 2022. *MtGSTF7*, a TT19-like GST gene, is essential for accumulation of anthocyanins, but not proanthocyanins in *Medicago truncatula*. *Journal of Experimental Botany* 73:4129–46

36. Goodman CD, Casati P, Walbot V. 2004. A multidrug resistance–associated protein involved in anthocyanin transport in *Zea mays*. *The Plant Cell* 16:1812–26

37. Francisco RM, Regalado A, Ageorges A, Burla BJ, Bassin B, et al. 2013. ABCC1, an ATP binding cassette protein from grape berry, transports anthocyanidin 3-*O*-glucosides. *The Plant Cell* 25:1840–54

38. Gomez C, Terrier N, Torregrosa L, Vialet S, Fournier-Level A, et al. 2009. Grapevine MATE-type proteins act as vacuolar H$^+$-dependent acylated anthocyanin transporters. *Plant Physiology* 150:402–15

39. Zhu Q, Xie X, Zhang J, Xiang G, Li Y, et al. 2013. *In silico* analysis of a MRP transporter gene reveals its possible role in anthocyanins or flavonoids transport in *Oryze sativa*. *American Journal of Plant Sciences* 4:555–60

40. Behrens CE, Smith KE, Iancu CV, Choe J, Dean JV. 2019. Transport of anthocyanins and other flavonoids by the Arabidopsis ATP-binding cassette transporter AtABCC2. *Scientific Reports* 9:437

41. Marinova K, Pourcel L, Weder B, Schwarz M, Barron D, et al. 2007. The *Arabidopsis* MATE transporter TT12 acts as a vacuolar flavonoid/H$^+$-antiporter active in proanthocyanidin-accumulating cells of the seed coat. *The Plant Cell* 19:2023–38

42. Pal L, Dwivedi V, Gupta SK, Saxena S, Pandey A, et al. 2023. Biochemical analysis of anthocyanin and proanthocyanidin and their regulation in determining chickpea flower and seed coat colour. *Journal of Experimental Botany* 74:130–48

43. Mathews H, Clendennen SK, Caldwell CG, Liu XL, Connors K, et al. 2003. Activation tagging in tomato identifies a transcriptional regulator of anthocyanin biosynthesis, modification, and transport. *The Plant Cell* 15:1689–703

44. Zhao J, Huhman D, Shadle G, He X, Sumner LW, et al. 2011. MATE2 mediates vacuolar sequestration of flavonoid glycosides and glycoside malonates in *Medicago truncatula*. *The Plant Cell* 23:1536–55

45. Shisa M, Takano T. 1964. Effect of temperature and light on the coloration of rose flowers. *Journal of the Japanese Society for Horticultural Science* 33:140–46

46. Hennayake CK, Kanechi M, Yasuda N, Uno Y, Inagaki N. 2006. Irradiation of UV-B induces biosynthesis of anthocyanins in flower petals of rose, *Rosa hybrida* cv. 'Charleston' and 'Ehigasa'. *Environmental Control in Biology* 44:103–10

47. Luo J, Li H, Bai B, Yu H, You J. 2013. Effect of light on the anthocyanin biosythesis and expression of *CHS* and *DFR* in *Rosa chinensis* 'Spectra'. *Molecular Plant Breeding* 11:126–31

48. Su M, Damaris RN, Hu Z, Yang P, Deng J. 2021. Metabolomic analysis on the petal of 'Chen Xi' rose with light-induced color changes. *Plants* 10:2065

49. Zhang Y, Wu Z, Feng M, Chen J, Qin M, et al. 2021. The circadian-controlled PIF8–BBX28 module regulates petal senescence in rose flowers by governing mitochondrial ROS homeostasis at night. *The Plant Cell* 33:2716–35

50. Wan H, Yu C, Han Y, Guo X, Luo L, et al. 2019. Determination of flavonoids and carotenoids and their contributions to various colors of rose cultivars (*Rosa* spp.). *Frontiers in Plant Science* 10:123

51. Wan H, Yu C, Han Y, Guo X, Ahmad S, et al. 2018. Flavonols and carotenoids in yellow petals of rose cultivar (*Rosa* 'Sun City'): a possible rich source of bioactive compounds. *Journal of Agricultural and Food Chemistry* 66:4171–81

52. Ren C, Chen C, Dong S, Wang R, Xian B, et al. 2022. Integrated metabolomics and transcriptome analysis on flavonoid biosynthesis in flowers of safflower (*Carthamus tinctorius* L.) during colour-transition. *PeerJ* 10:e13591

53. Han Y, Yu J, Zhao T, Cheng T, Wang J, et al. 2019. Dissecting the genome-wide evolution and function of R2R3-MYB transcription factor family in *Rosa chinensis*. *Genes* 10:823

54. Sun Y, Zhang X, Zhong M, Dong X, Yu D, et al. 2020. Genome-wide identification of *WD40* genes reveals a functional diversification of *COP1-like* genes in Rosaceae. *Plant Molecular Biology* 104:81−95

55. Ullah I, Yuan W, Uzair M, Li S, Rehman OU, et al. 2022. Molecular characterization of *bHLH* transcription factor family in rose (*Rosa chinensis* Jacq.) under *Botrytis cinerea* infection. *Horticulturae* 8:989

56. Li D, Li X, Liu X, Zhang Z. 2023. Comprehensive analysis of *bZIP* gene family and function of *RcbZIP17* on *Botrytis resistance* in rose (*Rosa chinensis*). *Gene* 849:146867

57. Geng L, Su L, Fu L, Lin S, Zhang J, et al. 2022. Genome-wide analysis of the rose (*Rosa chinensis*) *NAC* family and characterization of *RcNAC091*. *Plant Molecular Biology* 108:605−19

58. Liu X, Li D, Zhang S, Xu Y, Zhang Z. 2019. Genome-wide characterization of the rose (*Rosa chinensis*) *WRKY* family and role of *RcWRKY41* in gray mold resistance. *BMC Plant Biology* 19:522

59. Shalmani A, Fan S, Jia P, Li G, Muhammad I, et al. 2018. Genome identification of B-BOX gene family members in seven *Rosaceae* species and their expression analysis in response to flower induction in *Malus domestica*. *Molecules* 23:1763

60. Finn RD, Bateman A, Clements J, Coggill P, Eberhardt RY, et al. 2014. Pfam: the protein families database. *Nucleic Acids Research* 42:D222−D230

61. Wei L, Zhu Y, Liu R, Zhang A, Zhu M, et al. 2019. Genome wide identification and comparative analysis of glutathione trans-ferases (GST) family genes in *Brassica napus*. *Scientific Reports* 9:9196

62. Letunic I, Khedkar S, Bork P. 2021. SMART: recent updates, new developments and status in 2020. *Nucleic Acids Research* 49:D458−D460

63. Shao D, Li Y, Zhu Q, Zhang X, Liu F, et al. 2021. *GhGSTF12*, a glutathione S-transferase gene, is essential for anthocyanin accumulation in cotton (*Gossypium hirsutum* L.). *Plant Science* 305:110827

64. Katoh K, Standley DM. 2013. MAFFT multiple sequence alignment software version 7: improvements in performance and usability. *Molecular Biology and Evolution* 30:772−80

65. Kong Y, Wang H, Lang L, Dou X, Bai J. 2022. Effect of developmental stages on genes involved in middle and downstream pathway of volatile terpene biosynthesis in rose petals. *Genes* 13:1177

66. Chen C, Chen H, Zhang Y, Thomas HR, Frank MH, et al. 2020. TBtools: an integrative toolkit developed for interactive analyses of big biological data. *Molecular Plant* 13:1194−202

67. Jung S, Lee T, Cheng CH, Buble K, Zheng P, et al. 2019. 15 years of GDR: new data and functionality in the Genome Database for Rosaceae. *Nucleic Acids Research* 47:D1137−D1145

68. Daccord N, Celton JM, Linsmith G, Becker C, Choisne N, et al. 2017. High-quality *de novo* assembly of the apple genome and methylome dynamics of early fruit development. *Nature Genetics* 49:1099−106

69. de Vienne DM. 2016. Lifemap: exploring the entire tree of life. *PLoS Biology* 14:e2001624

70. Liu M, Xiao F, Zhu J, Fu D, Wang Z, Xiao R. 2023. Combined PacBio Iso-Seq and Illumina RNA-seq analysis of the *Tuta absoluta* (Meyrick) transcriptome and cytochrome P450 genes. *Insects* 14:363

71. Cheng C, Yu Q, Wang Y, Wang H, Dong Y, et al. 2021. Ethylene-regulated asymmetric growth of the petal base promotes flower opening in rose (*Rosa hybrida*). *The Plant Cell* 33:1229−51

72. Heberle H, Meirelles GV, da Silva FR, Telles GP, Minghim R. 2015. InteractiVenn: a web-based tool for the analysis of sets through Venn diagrams. *BMC Bioinformatics* 16:169

73. Szklarczyk D, Kirsch R, Koutrouli M, Nastou K, Mehryary F, et al. 2023. The STRING database in 2023: protein–protein association networks and functional enrichment analyses for any sequenced genome of interest. *Nucleic Acids Research* 51:D638−D646

74. Kong Y, Wang H, Lang L, Dou X, Bai J. 2021. Metabolome-based discrimination analysis of five *Lilium* bulbs associated with differences in secondary metabolites. *Molecules* 26:1340

75. Hennayake CK, Kanechi M, Uno Y, Inagaki N. 2007. Differential expression of anthocyanin biosynthetic genes in 'Charleston' roses. *Acta Horticulturae* 760:643−50

76. Lallement PA, Brouwer B, Keech O, Hecker A, Rouhier N. 2014. The still mysterious roles of cysteine-containing glutathione trans-ferases in plants. *Frontiers in Pharmacology* 5:192

77. Liu Y, Qi Y, Zhang A, Wu H, Liu Z, et al. 2019. Molecular cloning and functional characterization of *AcGST1*, an anthocyanin-related glutathione S-transferase gene in kiwifruit (*Actinidia chinensis*). *Plant Molecular Biology* 100:451−65

78. Li B, Zhang X, Duan R, Han C, Yang J, et al. 2022. Genomic analysis of the glutathione *S*-transferase family in pear (*Pyrus communis*) and functional identification of *PcGST57* in anthocyanin accumulation. *International Journal of Molecular Sciences* 23:746

79. Davis GV, Glover BJ. 2024. Characterisation of the R2R3 Myb subgroup 9 family of transcription factors in tomato. *PLoS ONE* 19:e0295445

80. Muñoz-Gómez S, Suárez-Baron H, Alzate JF, González F, Pabón-Mora N. 2021. Evolution of the subgroup 6 *R2R3-MYB* genes and their contribution to floral color in the perianth-bearing piperales. *Frontiers in Plant Science* 12:633227

81. Narbona E, del Valle JC, Arista M, Buide ML, Ortiz PL. 2021. Major flower pigments originate different colour signals to pollinators. *Frontiers in Ecology and Evolution* 9:743850

82. Ohashi K, Makino TT, Arikawa K. 2015. Floral colour change in the eyes of pollinators: testing possible constraints and correlated evolution. *Functional Ecology* 29:1144−55

83. Farzad M, Griesbach R, Weiss MR. 2002. Floral color change in *Viola cornuta* L. (Violaceae): a model system to study regulation of anthocyanin production. *Plant Science* 162:225−31

84. Rezende FM, Clausen MH, Rossi M, Furlan CM. 2020. The regulation of floral colour change in *Pleroma raddianum* (DC.) gardner. *Molecules* 25:4664

85. Ueda Y, Akimoto S. 2001. Cross- and self-compatibility in various species of the genus *Rosa*. *The Journal of Horticultural Science and Biotechnology* 76:392−95

86. Li M, Yang Y, Wang H, Fan Y, Sun P, et al. 2022. Identification and analysis of self incompatibility *S-RNase* in rose. *Acta Horticulturae Sinica* 49:157−65

87. Bursch K, Toledo-Ortiz G, Pireyre M, Lohr M, Braatz C, et al. 2020. Identification of BBX proteins as rate-limiting cofactors of HY5. *Nature Plants* 6:921−28

88. Li Y, Xu P, Chen G, Wu J, Liu Z, et al. 2020. FvbHLH9 functions as a positive regulator of anthocyanin biosynthesis by forming a HY5–bHLH9 transcription complex in strawberry fruits. *Plant and Cell Physiology* 61:826−37

89. Liu H, Su J, Zhu Y, Yao G, Allan AC, et al. 2019. The involvement of *PybZIPa* in light-induced anthocyanin accumulation via the activation of *PyUFGT* through binding to tandem G-boxes in its promoter. *Horticulture Research* 6:134

90. Zhao L, Sun J, Cai Y, Yang Q, Zhang Y, et al. 2022. *PpHYH* is responsible for light-induced anthocyanin accumulation in fruit peel of *Prunus persica*. *Tree Physiology* 42:1662−77

91. Bai S, Tao R, Tang Y, Yin L, Ma Y, et al. 2019. BBX16, a B-box protein, positively regulates light-induced anthocyanin accumulation by activating *MYB10* in red pear. *Plant Biotechnology Journal* 17:1985−97

92. Liu Y, Lin G, Yin C, Fang Y. 2020. B-box transcription factor 28 regulates flowering by interacting with constans. *Scientific Reports* 10:17789